Supplementary Material: Three Distinct Actin-attached Structural States of Myosin in Muscle Fibers

Ryan N. Mello and David D. Thomas*

Department of Biochemistry, Molecular Biology and Biophysics, University of Minnesota, Minneapolis, Minnesota

Section 1: RLC preparation and labeling

Chicken gizzard RLC (cgRLC) was used because (a) mechanics is preserved when cgRLC is exchanged for endogenous RLC in skinned rabbit psoas muscle(1), and (b) cgRLC contains a single Cys that enables specific spin labeling. The cgRLC was expressed in *E. coli,* purified as described previously (2,3), labeled at Cys108 with the cysteine-specific spin probe FDNASL (4), dissolved in labeling solution (50 mM NaCl, 2 mM EDTA, 20 mM EPPS, pH 8.0), and treated with 5 mM DTT for 1.5 hours. DTT was removed using two Zeba spin columns (Thermo Fisher Scientific Inc., Rockford, IL), protein concentration was adjusted to 100 μM, spin label was added at 500 μM, and the sample was incubated for 18-22 h on ice. Unreacted spin label was removed with a spin column equilibrated with Mg wash solution (40 mM NaCl, 2 mM $MgCl_2$, 10 mM EPPS, pH 8.0). If the FDNASL-RLC was not used within 1 day it was stored at -80^{o}C with 15% glycerol by volume. To simplify nomenclature, cgRLC is referred to as RLC in all other sections, other types of RLC are identified explicitly, and cgRLC labeled with the spin probe FDNASL is referred to as FDNASL-RLC.

The extent of spin labeling (spin labels per RLC) was determined both by digital analysis of EPR spectra (5) and by electrospray mass spectrometry (3). Briefly, for EPR analysis, the double integral of the V_1 spectrum of a known concentration of RLC (50 - 150 μM) was obtained at sufficiently low power to avoid saturation (typically < 1 mW). This value was then compared to the double integral of a sample of known spin label concentration (100 μM 2,2,6,6-Tetramethyl-1-piperidinyloxy (TEMPO)) at the same microwave power and H_1 value, to obtain the number of spin labels per RLC. For electrospray mass spectrometry, both unlabeled and labeled RLC (50 μM in 5mM ammonium bicarbonate solution) were injected into a QSTAR 2 quadrupole-TOF mass spectrometer with an electrospray ionization source. The resulting spectra were analyzed using Analyst QS software (Applied Biosystems). The area under peaks corresponding to unlabeled and labeled RLC were used to calculate the extent of spin labeling. The molar spin/protein ratio was 0.90 ± 0.08 determined from EPR analysis and 0.95 ± 0.01 determined from mass spectrometry, indicating essentially complete and specific reaction at Cys108.

Section 2: Nonspecific RLC binding

Previous work using EPR to measure LCD orientation indicated a significant fraction of nonspecific (largely disordered) RLC binding in skeletal muscle (4,7,8). We tested the hypothesis of nonspecific RLC binding in skeletal muscle fibers by incubating a fiber bundle in FDNASL-RLC, perfusing the fiber bundle with solution after incubation (to rinse away free FDNASL-RLC), and then using EPR to detect the presence of FDNASL-RLC. After rinsing away the free FDNASL-RLC, the fiber bundle had a significant EPR signal, V_{ns} (Fig. S1, C).

Since this fiber bundle did not have any of its native RLC extracted, and the EPR spectrum V_{ns} is indicative of random orientation, it is likely that the remaining exogenous FDNASL-RLC is bound nonspecifically. In an effort to minimize this nonspecifically bound RLC, we combined the RLC extraction and reconstitution steps. Previously, RLC extraction was followed by a separate reconstitution step (4,7-9). The purpose of combining the RLC extraction and reconstitution into one step is to extract the endogenous RLC and immediately replace it with FDNASL-RLC, while at the same time removing any FDNASL-RLC that binds nonspecifically. The functionally incorporated FDNASL-RLC, which binds very tightly, is not extracted by the extraction solution. A similar approach of including labeled RLC in the extraction solution was used previously in fluorescence studies (10,11).

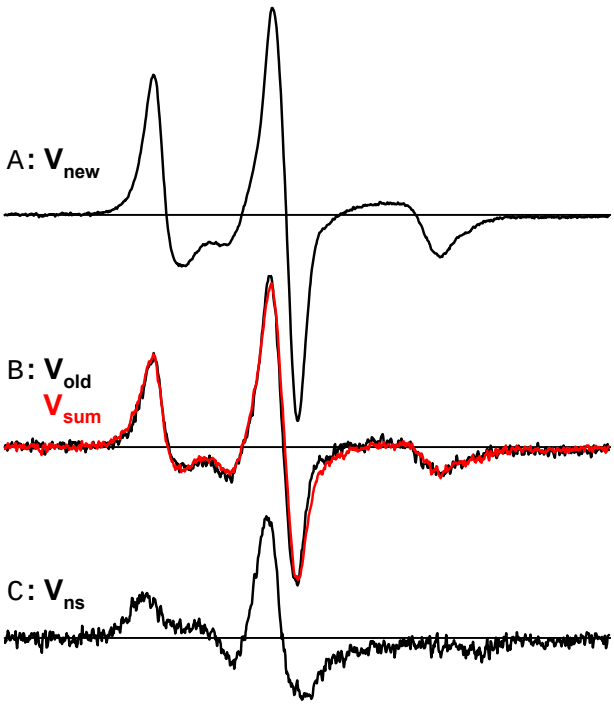

Fig. S1. EPR Spectra demonstrating a dramatic decrease in nonspecific RLC binding with the new RLC exchange procedure. Spectra were acquired in rigor with the fiber axis parallel to the field. A: Spectrum V_{new} from the new procedure, used in the current study. B: Spectrum V_{old} from the old procedure (9), overlaid on V_{sum} (red) that is the sum of 0.63 V_{new} + 0.37 V_{ns}. C: V_{ns} is the spectrum of nonspecifically bound spin-labeled RLC, as described in text.

The spectrum from fiber bundles treated with this new exchange procedure, V_{new} (Fig. S1A) is different from the spectrum of bundles treated with the old procedure, V_{old} (Fig. S1B). Based on a qualitative inspection of the spectra in Fig. S1, it is clear that the new procedure results in a much higher degree of orientation. We hypothesize that this is due to a decrease in the fraction of nonspecifically bound RLC, which is disoriented. If this hypothesis is true, it follows that V_{old} is a linear combination of V_{ns} and V_{new}, that is, a combination of nonspecifically bound and functionally incorporated RLCs,

$$V_{old} = V_{sum} = x_{ns}V_{ns} + (1-x_{ns})V_{new}$$

where x_{ns} = mole fraction of nonspecifically bound RLCs. Assuming this model, the best fit was obtained with $x_{ns} = 0.37$. The fit assuming this model is quite good (Fig. S1B) indicating that V_{old} is at least 37% V_{ns} (nonspecific RLC). Simulation of minced spectra (see EPR spectroscopy) indicates that V_{new} still contains a small amount (< 15%) of V_{ns}. This demonstrates that V_{old} is actually 52% V_{ns}, consistent with previous measurements (4), and the new exchange protocol (procedure below) reduces this to less than 15%.

Section 3: Method for RLC-exchange

Rabbit psoas fiber bundles were dissected from glycerinated strips into bundles measuring 0.3-0.5mm in diameter and 3–5 cm in length. Dissected bundles were then tied with silk thread at each end, and pulled into a glass capillary (25 µL Drummond Microdispenser, Drummond Scientific, Broomall, PA). The thread, and consequently the fiber bundle, were held stationary inside the capillary by capping the end of the capillary with silicone tubing. Thus the fiber bundle was held at a fixed length throughout RLC exchange, pPDM crosslinking, and EPR. The RLC exchange procedure was adapted from a previously described method (9), and is described below in seven steps. The 200 µL rinses were done one bundle at a time using a pipet to inject

solution through the capillary, otherwise a peristaltic pump (flow rate 0.5 mL/min) was used to perfuse the fiber bundles. Capillaries were connected in series when performing an RLC exchange on more than one fiber bundle.

1. Wash with pre-extraction solution (20 mM Imidazole, 20 mM KCl, 10 mM EDTA, 10 mM *trans*-1,2-Diaminocyclohexane-*N,N,N′,N′*-tetraacetic acid monohydrate (CDTA), 2 mM EGTA, pH 7.0), 10 min at 4°C.
2. Circulate ≥ 310 µL of extraction solution (pre-extraction solution with 10 mM 5, 5′-dithiobis (2-nitrobenzoic acid)(DTNB)) with FDNASL-RLC (≥ 0.6 mg/ml) over each fiber bundle, 10 min at 23°C.
3. Rinse three times with 200 µL of rigor solution 130 (RS130) (130 mM KPr, 2 mM $MgCl_2$, 1 mM EGTA, 20 mM MOPS, pH 7.0).
4. Incubate in RS130 (pH 8.0) with 30 mM DTT, 1.5 hours at 4°C.
5. Wash with RS130, 10 min at 4°C.
6. Incubate with 40 µL of RS130 + 5 mM MgATP + 4 mg/mL TnC, 1 hour at 4°C. After 1hr, add an additional 40 µL of TnC solution, and incubate for another hour at 4°C.
7. Rinse three times with 200 µL of RS130.

If the exchanged fiber bundles were not used immediately after exchange, they were placed in storage solution and stored at -20°C.

Section 4: SDS-PAGE

The extent of RLC extraction and reconstitution was determined by densitometric analysis of SDS-PAGE on fiber homogenates. Fiber homogenates were prepared by mechanically homogenizing muscle fibers with a PowerGen Model 125 homogenizer (Fisher Scientific, Pittsburgh, PA). Three fiber bundles (0.3-0.5mm in diameter and 3–5 cm in length) were homogenized in 375 µL of RS130 for 12 minutes using 15 s pulses alternating with 15 s pauses. After homogenization, 12 µg of fiber homogenate was loaded into an 18% Tris-HCl gel (Bio-Rad Laboratories). The gel was run at 200 V for 75 minutes. This is a longer run time than recommended by Bio-Rad, but we found that the lengthened run time improved separation between the RLC and TnC bands. Under these conditions endogenous RLC, FDNASL-RLC, TnC, ELC1, and ELC2 bands are well resolved (Fig. S2), making it possible to determine the relative amount of each protein. The extent of RLC extraction and reconstitution was calculated by comparing the ratio of the intensities of the endogenous RLC and FDNASL-RLC bands from the exchanged fiber homogenate (Fig. S2, lane 4) with the intensities from the control fiber homogenate (Fig. S2, lane 3). RLC intensities were normalized by the intensity of the ELC1 and ELC2 bands, as described previously (9,12). Since TnC is also extracted during the RLC exchange process, TnC was reconstituted after extraction. The extent of TnC reconstitution was determined using the same method used for the RLC. Densitometric analysis indicates that 54 ± 10 % of the endogenous RLC was extracted. After

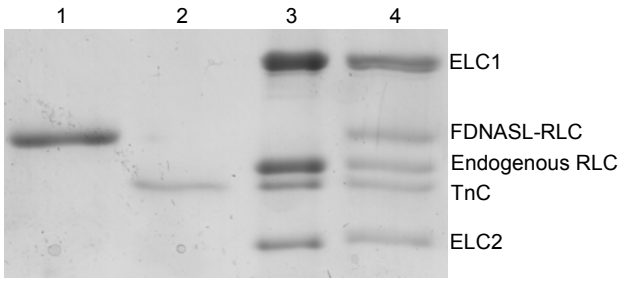

Fig. S2. 18% polyacrylamide gel showing protein composition of control and extracted muscle fiber homogenates. Lanes: (1) FDNASL-RLC, (2) purified rabbit skeletal TnC, (3) control muscle fiber homogenate, (4) exchanged muscle fiber homogenate.

reconstitution with FDNASL-RLC, the total RLC content was restored to 92 ± 3% relative to control values. TnC extracted during the exchange procedure was completely replaced.

Section 5: ATPase assays

Muscle fiber function after RLC exchange was assessed by measuring the Ca dependence of myofibrillar MgATPase activity, as measured with an NADH-enzyme linked microtiter plate assay (200 μL per well) in which the rate of oxidation of NADH is linked to the rate of ATP hydrolysis (13,14). Each well contained 50mM MOPS, 0.1 M KCl, 5mM $MgCl_2$, 1mM EGTA, 0.5 M phosphoenolpyruvate, 2.5 mM ATP, 0.2 mM NADH, 1 IU of pyruvate kinase, and 1 IU of lactate dehydrogenase. Myofibrils were prepared as described above (SDS-PAGE), except that the homogenization solution was 60mM KPr, 1 mM EGTA, 1 mM NaN_3, 25 mM MOPS, pH 7.0. The protein concentration was adjusted to 2mg/mL and combined (1:1 by volume) with sucrose solution (2 mM NaN_3, 0.6 M sucrose, 40mM MOPS, pH 7.0), and 10 μL of myofibril/sucrose solution was added to each well. The oxidation of NADH was followed by measuring the rate of decrease in absorption at 340 nm with a SpectraMax Plus 384 microplate reader (Molecular Devices). [Ca^{2+}] was controlled by EGTA buffering (15). The results were fitted with the Hill equation:

$$V = V_{max}/[1 + 10^{-n(pKCa - pCa)}], \qquad \text{Eq.1}$$

where V is the ATPase rate and n is the Hill coefficient. Control fiber bundles underwent a mock exchange, in which the extraction and reconstitution steps were replaced with RS130 washes in order to mimic the exchange procedure without extracting or reconstituting any protein.

To assess the modification of SH1 and SH2, the K/EDTA and Ca/K ATPase activities of myofibrils were measured at high ionic strength by measuring phosphate liberation after acid quench (16). The incubation solution (25°C) contained 0.6M KCl, 50 mM MOPS, and 10 mM of either EDTA (K/EDTA ATPase) or $CaCl_2$ (Ca/K ATPase) (pH 7.5). Myofibrils were prepared using the same method as described above (SDS-PAGE), except the fibers were homogenized in a solution of 10 mM MOPS. Using a previously described method (17), the fraction of crosslinked heads was calculated using the K/EDTA and Ca/K ATPase activities from control and crosslinked fibers.

Fig. S3

Simulations (Fig. S3) illustrate the dependence of EPR spectra on θ′ when the fiber axis is aligned parallel (red, θ′ = θ) and perpendicular (blue, where θ′ exhibits more disorder due to helical symmetry of the muscle fiber) to H (17).

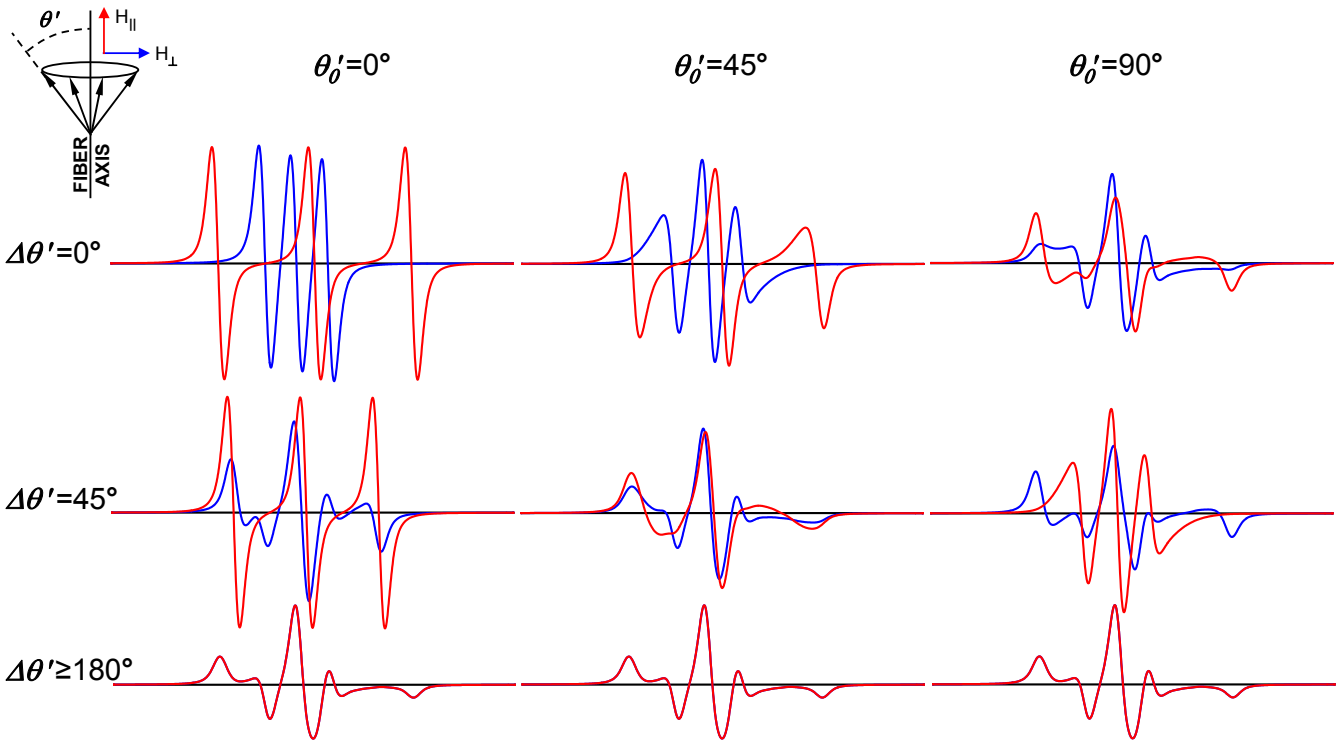

Fig. S3. Simulated EPR spectra showing dependence of conventional EPR (V_1) on tilt angle θ′ of the spin label principal axis relative to the muscle fiber axis. A Gaussian distribution of θ′ is assumed, where θ_0' is the center of the distribution and Δθ′ is the full width at half-maximum. Spectra correspond to the muscle fiber axis oriented parallel (red) and perpendicular (blue) to the applied magnetic field (H). The difference between red and blue provides a clear indication of the degree to which the protein is oriented relative to the muscle fiber axis. In the bottom row, corresponding to complete disorder, there is no difference between red and blue, so blue is not visible.

Fig. S4
In addition to being sensitive to orientation, EPR is sensitive to rotational dynamics on the timescale of picoseconds to microseconds (18).

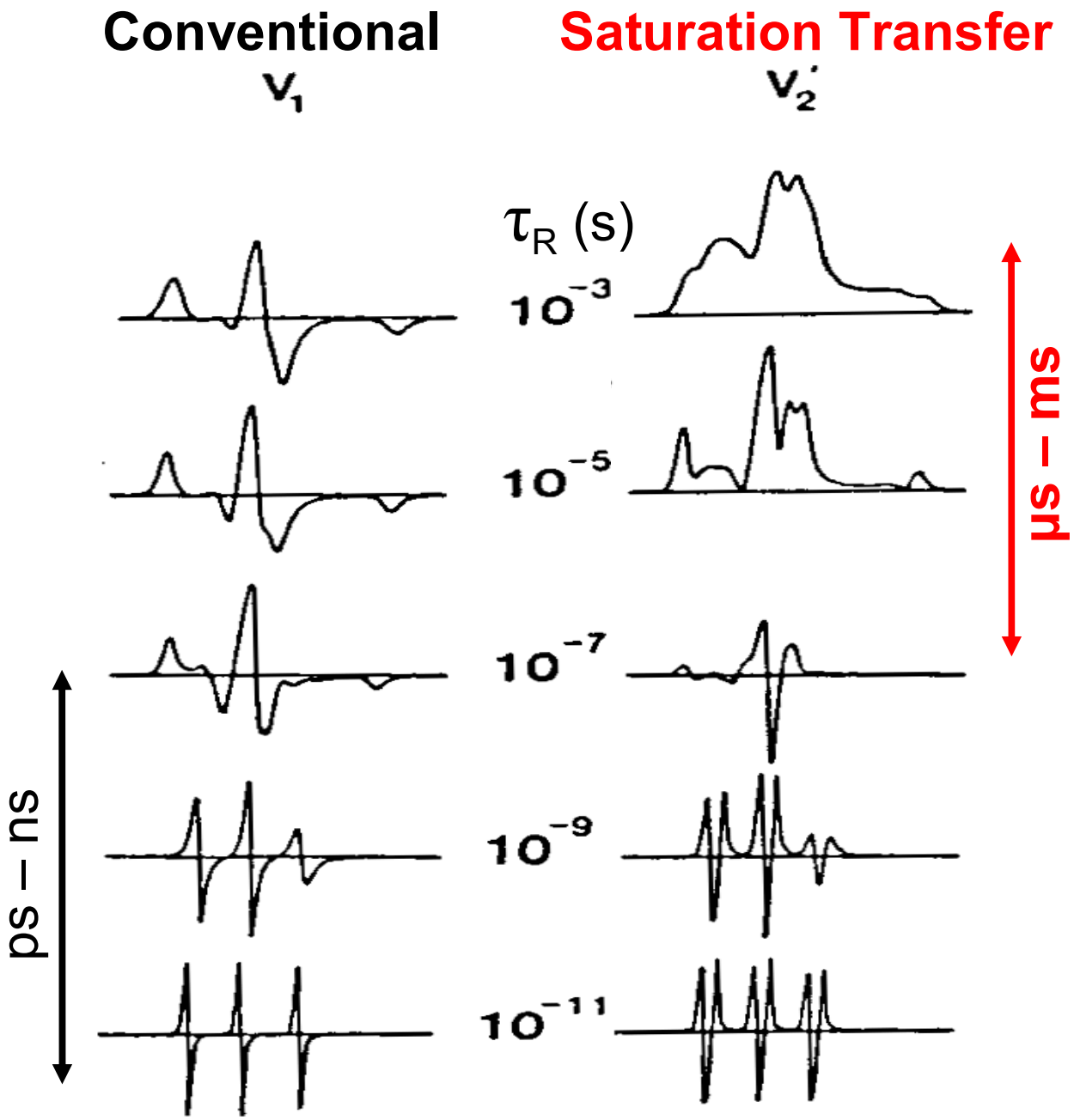

Fig. S4. Sensitivity of conventional (V_1, left) and saturation transfer (V_2', right) EPR spectra to rotational dynamics of nitroxide spin labels. V_1 spectra are sensitive only to submicrosecond rotational correlations times (τ_R), while V_2' spectra are sensitive to much slower motions. Adapted from (17).

REFERENCES

1. Ling, N., C. Shrimpton, J. Sleep, J. Kendrick-Jones, and M. Irving. 1996. Fluorescent probes of the orientation of myosin regulatory light chains in relaxed, rigor, and contracting muscle. Biophys J 70:1836-1846.

2. Nelson, W. D., S. E. Blakely, Y. E. Nesmelov, and D. D. Thomas. 2005. Site-directed spin labeling reveals a conformational switch in the phosphorylation domain of smooth muscle myosin. Proc Natl Acad Sci U S A 102:4000-4005.

3. Kast, D., L. M. Espinoza-Fonseca, C. Yi, and D. D. Thomas. 2010. Phosphorylation-induced structural changes in smooth muscle myosin regulatory light chain. Proc Natl Acad Sci U S A 107:8207-8212.

4. Baker, J. E., I. Brust-Mascher, S. Ramachandran, L. E. LaConte, and D. D. Thomas. 1998. A large and distinct rotation of the myosin light chain domain occurs upon muscle contraction. Proc Natl Acad Sci U S A. p 2944-2949.

5. Karim, C. B., Z. Zhang, and D. D. Thomas. 2007. Synthesis of TOAC spin-labeled proteins and reconstitution in lipid membranes. Nat Protoc 2:42-49.

6. Prochniewicz, E., D. A. Lowe, D. J. Spakowicz, L. Higgins, K. O'Conor, L. V. Thompson, D. A. Ferrington, and D. D. Thomas. 2008. Functional, structural, and chemical changes in myosin associated with hydrogen peroxide treatment of skeletal muscle fibers. Am J Physiol Cell Physiol 294:C613-626.

7. Hambly, B., K. Franks, and R. Cooke. 1991. Orientation of spin-labeled light chain-2 exchanged onto myosin cross-bridges in glycerinated muscle fibers. Biophys J 59:127-138.

8. Hambly, B., K. Franks, and R. Cooke. 1992. Paramagnetic probes attached to a light chain on the myosin head are highly disordered in active muscle fibers. Biophys J 63:1306-1313.

9. Roopnarine, O. 2003. Mechanical defects of muscle fibers with myosin light chain mutants that cause cardiomyopathy. Biophys J 84:2440-2449.

10. Corrie, J. E., B. D. Brandmeier, R. E. Ferguson, D. R. Trentham, J. Kendrick-Jones, S. C. Hopkins, U. A. van der Heide, Y. E. Goldman, C. Sabido-David, R. E. Dale, S. Criddle, and M. Irving. 1999. Dynamic measurement of myosin light-chain-domain tilt and twist in muscle contraction. Nature 400:425-430.

11. Burghardt, T. P., K. Ajtai, D. K. Chan, M. F. Halstead, J. Li, and Y. Zheng. 2007. GFP-tagged regulatory light chain monitors single myosin lever-arm orientation in a muscle fiber. Biophys J 93:2226-2239.

12. Moss, R. L., G. G. Giulian, and M. L. Greaser. 1982. Physiological effects accompanying the removal of myosin LC2 from skinned skeletal muscle fibers. J Biol Chem 257:8588-8591.

13. Madden, T. D., D. Chapman, and P. J. Quinn. 1979. Cholesterol modulates activity of calcium-dependent ATPase of the sarcoplasmic reticulum. Nature 279:538-541.

14. Karim, C. B., M. G. Paterlini, L. G. Reddy, G. W. Hunter, G. Barany, and D. D. Thomas. 2001. Role of cysteine residues in structural stability and function of a transmembrane helix bundle. J Biol Chem 276:38814-38819.

15. Fabiato, A. and F. Fabiato. 1979. Calculator programs for computing the composition of the solutions containing multiple metals and ligands used for experiments in skinned muscle cells. J Physiol (Paris) 75:463-505.

16. Lanzetta, P. A., L. J. Alvarez, P. S. Reinach, and O. A. Candia. 1979. An improved assay for nanomole amounts of inorganic phosphate. Anal Biochem 100:95-97.

17. Thompson, A. R., N. Naber, C. Wilson, R. Cooke, and D. D. Thomas. 2008. Structural dynamics of the actomyosin complex probed by a bifunctional spin label that cross-links SH1 and SH2. Biophys J 95:5238-5246.

18. Thomas, D. D., L. R. Dalton, and J. S. Hyde. 1976. Rotational diffusion studied by passage saturation transfer electron paramagnetic resonance. J Chem Phys 65.